Temperature anomalies of hypersound velocity and specific heat ratio in liquid Quinoline

Louis Letamendia[a], Miad Belkadi[a], Omar Eloutassi[a], Jacques Rouch[a], Dino Risso[b], Patricio Cordero[c], Alexander Z. Patashinski[d,*]

[a]*Centre de Physique Moléculaire Optique et Hertzienne, UMR5798 du CNRS Université Bordeaux 1, 351 Cours de la Libération 33405 Talence, France*
[b]*Departamento de Fisica, Universidad del Bio Bio Collao 1202 Concepcion, Chile*
[c]*Departamento de Fisica Universidad de Chile, Blanco Encalada 2008 Santiago, Chile*
[d]*Department of Chemistry and Materials Research Center, Northwestern University, Evanston, IL 60208, USA*

Abstract

Results of an extensive study of dynamic polarized (VV) and depolarized (VH) Rayleigh–Brillouin light scattering in Quinoline as a function of temperature are presented. The VV spectrum is analyzed by taking into account the fine structure (shear dip) of the VH spectrum. The hypersound velocity $u(T)$ and the Landau–Placzek ratio $\gamma(T)$ have been calculated from the frequency shift of the Brillouin lines and the ratio of the integrated intensities of the non-shifted Rayleigh line to the two Brillouin lines. Under the conditions of high-purity and long equilibration times, the temperature variations of both $u(T)$ and $\gamma(T)$ show two reproducible anomalies centered at about 17 and 42 °C. We discuss an interpretation of the anomalies based on local structure changes, and possible relations of these anomalies to liquid–liquid phase transitions in equilibrium liquids.

Keywords: Complex liquids; Local order; Brillouin scattering; Liquid–liquid phase transitions

*Corresponding author. Department of Physics and Astronomy, Northwestern University, 2145 Sheridan Road, Evanston, IL 60208-3112, USA. Fax: +1 847 491 9982.

E-mail address: patashin@casbah.it.northwestern.edu (A.Z. Patashinski).

1. Introduction

Far from the melting line, high-temperature liquids are well described by a model of a structure-less fluid; at lower temperatures, and especially at supercooling, the properties of liquids may be explained using the concept of local structure in liquids [1,2]. In these low-temperature liquids, relaxation processes are thermally activated. The activation energy may be found from viscosity dependence on temperature. Most of the effects related to the local structure are found in supercooled liquids close to the glass transition, where the activation energy is much larger than the thermal energy k_BT. For many systems, this energy substantially increases upon cooling towards the glass transition. It is generally believed that this super-Arrhenius behavior reflects monotonous and continuous changes in the local structure of the liquid upon cooling.

The effects related to the local structure are not limited to the supercooled state of liquids. Recent studies of equilibrium liquids found discontinuities in the temperature dependence of electrical conductivity and heat capacity [3–6] in molten sulfur, selenium, iodine, bismuth, and tellurium. These discontinuities were interpreted, following the earlier theory [3–10], in terms of changes in the local order due to a phase transition between liquid states differing in local structure.

The continuous and monotonous properties change, and discontinuities at a liquid–liquid phase transition are two limits of ordering behavior in statistical mechanics. The liquid–liquid transition between liquid states with different local structure assumes [7,8] the existence of competing local structure types in the system (polyamorphism). Note that, unlike the liquid crystalline ordering, in the continuous properties change as well as the discontinuous change in liquid–liquid phase transitions the global symmetry of the liquid is not changed. The liquid–liquid phase transition line terminates at the critical point; crossing of the phase transition line closer and closer to this point will result in diminishing discontinuities, and increase of fluctuations. In the supercritical range of parameters, only non-monotonous properties change remains as an indication of rapid changes in the statistics of competing local structures upon cooling. One may suggest that anomalies (non-monotonous behavior upon temperature change) in liquids manifesting changes in the local structure are common phenomena for low-temperature liquids with competing local structures. We believe that the unexpected physical behaviors found in Benzene, Quinoline, and other complex fluids [11–18], are manifestations of changes in the local structure, and that similar phenomena may be observed, under special experimental conditions, in many equilibrium and supercooled liquids. The magnitudes of the observed effects are small, and special care has to be given to the purity of the liquids and equilibration time. In particular, a very careful de-gassing is a necessary condition for the observation of the effect. The anomalies of behavior were so far observed in the hypersound velocity and the ratio of the isobaric and isochoric heat capacities. In Quinoline and Benzene, the orientation relaxation times of molecules were shown to increase with increasing temperature in small temperature domains located well above the freezing point [18].

A liquid characterized by a long-living local structure may have new slow modes that are beyond the framework of the classical theory of liquids. In low-temperature liquids consisting of rotationally asymmetric molecules, a new hydrodynamic mode of molecular rotation was long ago predicted by Leontovich [19], and experimentally confirmed by Fabelinskii [20]. In a Leontovich liquid, a change of molecular orientation beyond the small thermal vibrations is a relaxation process characterized by a relaxation time $\theta_{or} \gg \tau$, where τ is the microscopic period of molecular vibrations; usually, $\tau \sim 10^{-12}$–10^{-11} s. The orientation relaxation is coupled to the momentum density in the modified set of hydrodynamic equations. More recently, Kawasaki [21] assumed the existence of many new modes neglected in classical theories. Theoretical models based on the slow mode assumption have been proposed by Mountain et al. [22], and Oxtoby et al. [23]. Kivelson et al. [24,25] developed a frustrated transition scenario that includes a slow mode.

In the current paper, we report new results of a study of light scattering in Quinoline. In previous experiments, an unusual behavior of the temperature variation of the hypersound velocity in Benzene and Hexafluorobenzene [17] was found at typically $\sim$5 GHz from the shift of the Brillouin doublet in polarized Rayleigh–Brillouin spectra. In Quinoline and Benzene, abnormal behavior has also been evidenced [18] in the reorientation correlation time inferred from the width of the depolarized Rayleigh spectra. In contrast to the expected monotonic change with temperature, these quantities have reproducible anomalies at 36 and 46 °C for Benzene, and 38 and 50 °C for Hexafluorobenzene, well above the freezing temperatures of these liquids.

We present the temperature dependence of the hypersound velocity u and of the specific heats ratio γ derived from extensive measurements of the polarized and depolarized Rayleigh–Brillouin spectra in liquid Quinoline. Both quantities show anomalies at temperatures close to 17 and 42 °C. The reorientation relaxation time and the spin–lattice relaxation time T_1 of Quinoline have anomalies [14,15,18,26] at the same temperatures. A plausible interpretation of the observed anomalies in terms of orientation ordering and a possible relation of these anomalies to liquid–liquid phase transitions are discussed in the last section. Based on known characteristics of interaction in the systems, we make suggestions about the ordering in the liquid manifested by the anomalies observed. More work is needed to yield a clear understanding of the details of these ordering processes.

2. Experimental

Quinoline from Fluka, contained in a cylindrical sealed glass cell (scattering cell), was first triply distillated under vacuum to eliminate dust, then submitted to freezing cycles in order to remove dissolved gases. The polarized light from a 2020 Argon Spectra Physics Ion laser delivering a longitudinal single-mode radiation at 514.5 nm is focused on the scattering cell that is imbedded in a circulating bath containing a

liquid of high refractive index to insure index matching. The temperature of the bath is stable at better than ± 0.01 K during the duration of the experiment. Mirrors allow us to vary the scattering angle θ from 30° up to 150°. The scattering wave-vector

$$k = \frac{4\pi n}{\lambda} \sin\left(\frac{\theta}{2}\right)$$

is then changed by a factor of almost 4. Here, n is the refractive index of the sample and λ the wavelength of the laser light. One can measure the VV, VH, HV and HH spectra by using a polarization rotator mounted on the laser head, and polarizers located on the scattered beam. Here, V means that the beam is polarized perpendicular to the scattering plane (vertical direction), and H refers to the polarization parallel to the scattering plane (horizontal direction). In the current paper, we shall focus on the polarized VV and depolarized VH spectra. The scattered light is analyzed by using a Tropel double-pass plane Fabry–Pérot interferometer (FP). To avoid fluctuations of the refractive index of the air between the coated plates, the (FP) is located in a temperature-controlled housing. The light issued from the FP is focused on a pinhole of convenient diameter and then received via an optical fiber on an avalanche diode working in Geiger regime with a quantum efficiency of nearly 50%.

In order to account for possible frequency drift of the laser frequency during the experiment, the electronic scanning procedure of the FP is as follows. The parallelism of the plates of the FP is adjusted by piezoelectric transducers (PZT) connected to a tunable high voltage power supply. This allows us both to adjust the alignment of the plates at the beginning of the experiment and to maximize the finesse coefficient (typically 50) during all the duration of the experiment via a feedback system. For that task, the FP is alternatively illuminated by the scattered beam and by a second beam of very low intensity directly coming from the laser. During each scan corresponding to two interference orders of the FP, the signal corresponding to the direct beam is maximized by acting on the PZT transducers and recorded. Then the scattered beam is recorded in his turn. All the data are accumulated on a 1024 channels multi-channel analyzer driven by a PC computer via a National Instrument card. For each experiment, we measure both the instrumental function during the total duration of the experiment (typically 1 H), and the scattered spectrum. Then, the scattered spectra are deconvoluted using Zamir et al. [27] procedure. It has to be stressed that, due to polarization selection rules in dynamical light scattering, the VV spectrum is the sum of the totally polarized Rayleigh–Brillouin triplet (dynamical structure factor $S(k,\omega)$, where ω is the cyclic frequency) and of a part of the intense depolarized VH spectrum [28,29]. It is easy to show that the VV spectrum intensity distribution $I_{VV}(k,\omega)$ is given by $I_{VV}(k,\omega) = S(k,\omega) + (3/4)I_{VH}(k,\omega)$, where $I_{VH}(k,\omega)$ represents the intensity distribution of the VH depolarized spectrum. Therefore, in order to have a precise measurement of $S(k,\omega)$ one has to carefully account for the VH spectrum. This spectrum was also recorded. To describe the shape of the VH spectrum, we used the most recent model, proposed by Quentrec [30], that accounts for the coupling between the reorientation motion of

molecules and dissipative shear waves:

$$I_{VH}(k,\omega) = \sin^2\frac{\theta}{2}\frac{\Gamma}{\omega^2+\Gamma^2} + \cos^2\frac{\theta}{2}\frac{\Gamma\left(\omega^2+\eta_0\eta_\infty\dfrac{k^4}{\rho^2}\right)}{\left(\omega^2-\eta_0\dfrac{\Gamma k^2}{\rho}\right)^2+\omega^2\left(\Gamma+\eta_\infty\dfrac{k^2}{\rho}\right)^2}. \quad (1)$$

In formula (1), Γ is the reorientation relaxation frequency of molecules, ρ is the density; η_0 and $\eta_\infty = \eta_0(1-R)$ are, respectively, the low- and high-frequency values of the shear viscosity, R being a coupling constant ($0<R<1$). In most cases, R is about 0.4. A typical fit of the VH spectrum to Eq. (1) is shown in Fig. (2). As one can see, a very good fit of the experimental data using Eq. (1) may be achieved.

For non-relaxing liquids, the analytic expression for the dynamical structure factor $S(k,\omega)$ has been deduced by many authors in the form

$$S(k,\omega) = \left(\frac{\gamma-1}{\gamma}\right)\frac{\Gamma_C}{\omega^2+\Gamma_C^2} + \frac{1}{2\gamma}\left[\frac{\Gamma_B}{(\omega-\Omega_B)^2+\Gamma_B^2} + \frac{\Gamma_B}{(\omega+\Omega_B)^2+\Gamma_B^2} - \frac{\Gamma_B(\omega-\Omega_B)}{(\omega-\Omega_B)^2+\Gamma_C^2} + \frac{\Gamma_B(\omega+\Omega_B)}{(\omega+\Omega_B)^2+\Gamma_C^2}\right], \quad (2)$$

$S(k,\omega)$ is the sum of a non-shifted central Rayleigh line and two symmetrically shifted Brillouin lines. The Rayleigh line is a Lorentzian line accounting for thermal dissipation in the liquid. The two shifted Brillouin lines are a Lorentzian line and an anti-Lorentzian line. In the formula (2), Ω_B is the Brillouin frequency, Γ_C and Γ_B are, respectively, the half-widths at half-high of the central Rayleigh line and of the Brillouin lines. These quantities are related to transport coefficients of the liquid, the thermal conductivity and shear and bulk viscosities. The quantity γ is the ratio of specific heats at the constant pressure and constant volume. This quantity can be found by measuring the ratio R_{LP} of integrated intensities of the central Rayleigh line I_C to the two Brillouin lines $2I_B$:

$$R_{LP} = \frac{I_C}{2I_B} = \gamma - 1. \quad (3)$$

The Brillouin frequency shift Ω_B is related to the sound velocity u by $\Omega_B = ku$. In fact, in a Brillouin scattering experiment the wave-vector k is fixed by experimental conditions. In the case of ultrasonic experiments that give directly u, the frequency is fixed. Therefore, the measured quantity in a Brillouin scattering experiment is not exactly u but u_∞. These two quantities are linked by

$$u_\infty \approx u\left(1+\frac{\Gamma_B^2}{2\Omega_B^2}\right). \quad (4)$$

As we shall see below, the correction for the sound velocity is of the order of 2%. Experimental interferograms for polarized VV (triangles) and depolarized VH (squares) Rayleigh–Brillouin spectra, recorded at the same temperature 45 °C and wave-vector, are depicted in Fig. 1. The VH spectrum, clearly showing the so-called

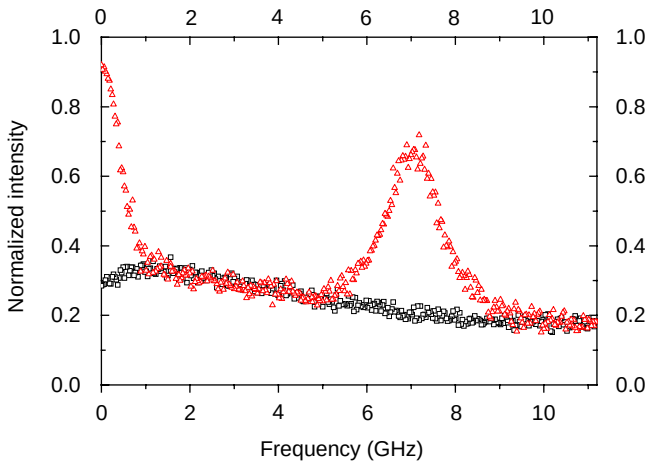

Fig. 1. Polarized spectrum $I_{VV}(q,\omega)$ (triangles) and depolarized spectrum $I_{VH}(q,\omega)$ (squares) in Quinoline at 45 °C. Apparatus functions are the same in both measurements.

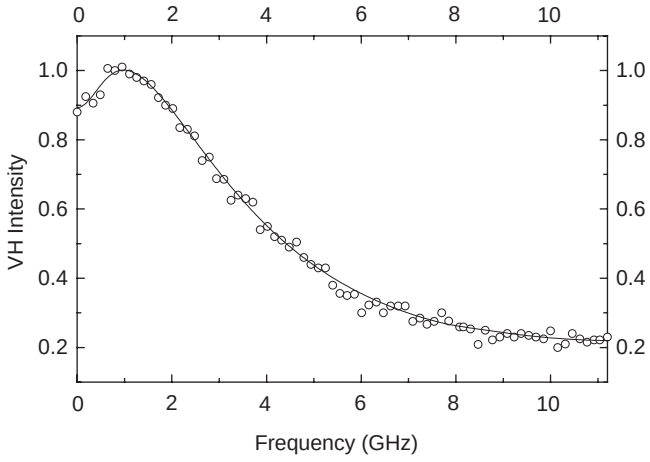

Fig. 2. Depolarized spectrum $I_{VH}(q,\omega)$: experimental data (circles) and the fit using formula (1) (continuous line).

shear dip, is so intense that an incorrect evaluation may result in an error in the parameters involved in $S(k,\omega)$ of more that 20%. A typical fit of the VH spectrum, obtained at 15 °C to Quentrec model [30], is shown in Fig. 2.

A good agreement between our experiments and the model is achieved at temperatures ranging from 10 to 60 °C. Using VH data, one can fit the experimental VV spectrum; a typical fit is shown in Fig. 3. Here, a very good agreement is also observed between the experimental data and the theoretical model. From the fit, we obtain the dynamic structure factor $S(k,\omega)$ and the relevant parameters, the sound velocity u and the Landau–Placzek ratio R_{LP}. The experimental error for the sound

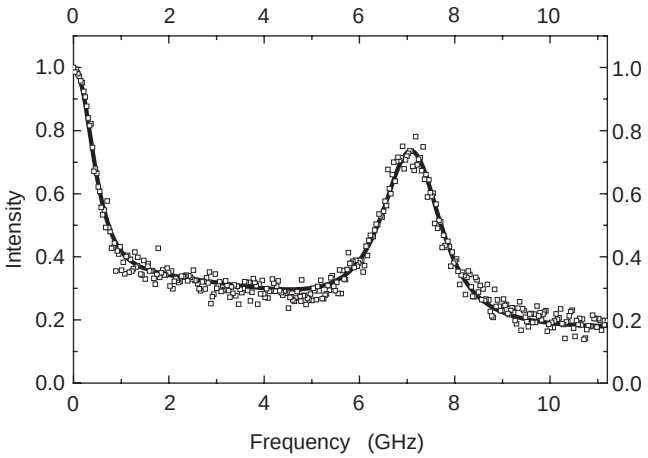

Fig. 3. A typical polarized spectrum $I_{VV}(q,\omega)$: experimental data (squares) and the fit using formula (5) (continuous line).

velocity u is of the order of $\pm 0.5\%$, or $\sim 7.5\,\mathrm{ms}^{-1}$, whereas the experimental error for $\gamma = R_{LP} + 1$ is about $\pm 5\%$. The formula for the intensity I_{VV} may be written as

$$I_{VV}(k,\omega) = \frac{\gamma-1}{\gamma}\frac{2\Gamma_C}{\omega^2+\Gamma_C^2} + \frac{1}{\gamma}\left[\frac{\Gamma_B}{(\omega-\Omega_B)^2+\Gamma_B^2} - \frac{(\Gamma_B+(\gamma-1)\Gamma_C)(\omega-\Omega_B)}{(\omega-\Omega_B)^2+\Gamma_B^2} + \frac{\Gamma_B}{(\omega+\Omega_B)^2+\Gamma_B^2} + \frac{(\Gamma_B+(\gamma-1)\Gamma_C)(\omega+\Omega_B)}{(\omega+\Omega_B)^2+\Gamma_B^2}\right]. \quad (5)$$

3. Experimental results

The experimental results critically depend on the degree of liquid purification, especially degassing, and on equilibration time preceding the measurement of the spectrum. We assume that this high sensitivity of the results to preparation factors is an important feature to help in interpretation of the obtained data. Fig. 4 shows the sound velocity as a function of temperature for triply distillated and de-gazed Quinoline samples prepared as described above (full dots). On the same graph, we have also plotted the sound velocity deduced for Quinoline taken from the pot and only filtered on Millipore filters to eliminate dust (full line). Whereas in filtered Quinoline we observe the classical monotonic quasi-linear decrease of the sound velocity upon increasing temperature, a non-monotonic behavior is observed for triply distillated Quinoline. The sound velocity shows two well-defined local maxima at temperatures about 17 and 42 °C. The maxima are very well reproducible and cannot be attributed to experimental errors. Indeed, the amplitude of the two humps is of the order of $50\,\mathrm{m\,s}^{-1}$ while the experimental uncertainty is less than $\pm 10\,\mathrm{m\,s}^{-1}$.

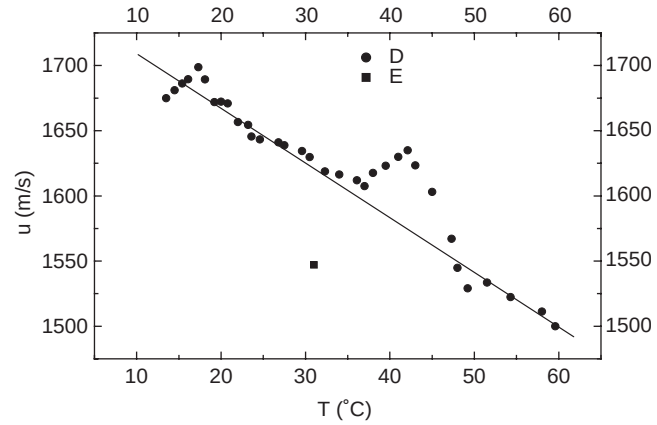

Fig. 4. Sound velocity u as a function of temperature: neat Quinoline (black disks), and usual grade (not neat) Quinoline (continuous line). The black square shows the data of one ultrasound measurement.

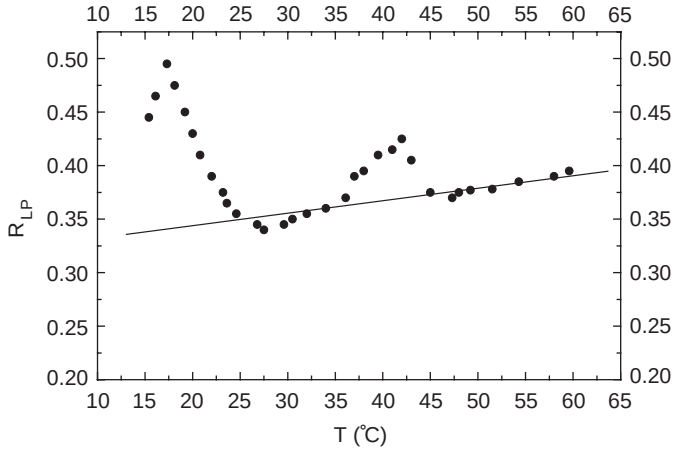

Fig. 5. The Landau–Plazek ratio R_{LP} as a function of temperature in Quinoline. Data for the neat system (squares) and for the not neat Quinoline (continuous line).

On the same graph, we have also plotted the sound velocity found in an ultrasound experiment (full square). Acoustic measurements have been performed at only one temperature, located in the "normal liquid" regime. The observed large dispersion of the sound velocity (of the order of $150\,\mathrm{m\,s^{-1}}$) indicates that there are relaxation modes in the frequency range between the ultra- and hypersound. These relaxation modes are expected to result in the Mountain lines centered at the zero (laser) frequency. In our measurements, we have been unable to measure these lines since they are hidden by the intense non-shifted Rayleigh line and by the depolarized VH line.

Fig. 5 shows the ratio $R_{LP} = I_C/2I_B$ of the integrated intensities of the central Rayleigh line I_C to the two Brillouin lines $2I_B$. According to the Landau–Placzek

theory, $R_{PL} = \gamma - 1$, where $\gamma = C_P/C_V$ is the ratio of heat capacities at constant pressure and volume. Note that R_{LP} can be accurately evaluated only if the VH spectrum is taken into account. In Fig. 5, full dots show this ratio, deduced from the values of R_{LP}, for the triple cleaned Quinoline, while the full line gives the behavior of γ for filtered only Quinoline where the change of γ with temperature is quite small. Within the accuracy of the experiment (typically $\pm 5\%$), γ shows two humps at the same temperatures 17 and 42 °C as the sound velocity u. This allows one to conclude that the anomalies in both u and γ have a common physical origin.

4. Discussion, and interpretation of the experimental data

Anomalies with similar manifestations seem to be a quite general phenomenon in complex and glass-forming liquids when sufficient experimental care is taken. For instance, anomalies have been observed above the melting temperature in Benzene [16–18], Quinoline, Hexafluorobenzene [16,17], and some other related (aromatic) liquids. One may also include in this list non-aromatic compounds, for example Glycerol [31]. The conditions of observation of the anomalies include unusually high purity of the sample, and long relaxation times. One may suggest that these anomalies share a common mechanism, and represent a rather general phenomenon of weak ordering, although not yet well studied and understood. We therefore believe that, when the special observation conditions are met, many complex liquids at low temperatures will show similar anomalies.

Complex liquids are, by definition, liquids in which the physical properties show a significant contribution of fluctuating molecular arrangement (referred to as local order). It seems to us naturally to assume that the observed anomalies are thermodynamic and kinetic manifestations of changes in the local order with temperature changes. The observed large dispersion of the sound velocity may be linked to these changes [32]. The details of the general mechanism in a specific system have to be concretized by taking into account the features of the molecules and their interaction, determined by the chemical structure of the molecules. What has to be understood is not only the form of the anomalies, but also the high sensitivity of the experimental results to impurities, specifically to small amounts of dissolved gases, and the large equilibration time required to achieve reproducibility. These last conditions may provide a hint for the interpretation of the effects observed. In the present paper, we shall limit our discussion to aromatic liquids.

Anomalies observed in Benzene [16–18] include maxima in hypersound velocity, orientation relaxation time, and the ratio $\gamma = C_P/C_V$ as functions of temperature. There are two relatively close temperatures where these maxima occur, 35 and 50 °C. For Quinoline, neutron scattering experiments by Bermejo et al. [14] evidenced an unusual correlation around 17 °C. In the same liquid, NMR measurements performed by Robert et al. [15] show a detectable structural change at the same temperature. In these publications, a change of the molecular arrangement upon cooling/heating is suggested as the cause of the observed effects. While we accept this general point of view, the task remains to explain, based on molecular level analysis,

the nature of this change. Below, we shall suggest a physical picture of low-temperature aromatic liquids that may explain observed anomalies and some other physical properties of these systems. This picture is based on assumptions that need to be tested by future experiments.

The molecules of Benzene, Quinoline, and Hexafluorobenzene share features common for aromatic molecules [33]. For considerations related to the structure of the liquid, these molecules may be treated as plain and rigid bodies without internal degrees of freedom. The relatively rigid electronic configurations of the molecules are characterized by a significant separation of positive and negative electric charges at the molecular length scale of few Angstroms. At very short distance between molecules, strong repulsion determines the shapes of the molecules; and at the only slightly larger length-scale, attraction become important. At this distance, the electric charge distribution may be characterized in terms of rigid electrical multipoles. Interactions of these multipoles, together with the very short-range repulsion, determine the set of mutual positions and orientations of two neighboring molecules corresponding to potential energy minima. Dispersion forces are less sensitive to structure, and mostly favor higher densities of the liquid.

In gas state at temperatures of the anomalies (close to the triple point), the binding energies ΔE supporting the dimers, as well as the energy barriers for switching between dimer configurations, are only 3–10 times the thermal energy $k_B T$ in Benzene; the energies ΔE for the most stable dimer configurations increase with increasing number of aromatic rings in the molecule. The position entropy s that is lost when two molecules dimerize is $s \sim k_B \ln v$, where v is the free volume per molecule. This volume is large in the gas state, so that dimers easily break up (evaporate), and the relative concentration of dimers is small. In the low-temperature liquid state, the density is high and v is small, so that both the positional and orientational parts of the entropy are of the same order, and $s \sim \Delta E/T$. Then, the probability to find two neighboring molecules in relative positions and orientations near a minimum of the interaction energy becomes significant. To distinguish the situation when two neighboring molecules are close to one of the minima of the pair interaction energy, we will refer to those two molecules as paired. We expect that in the temperature range of the anomalies, a molecule frequently pairs with more than one neighbor. This creates an ordered cluster with correlation in positions and orientations of the molecules in this cluster.

A description of a liquid in terms of pairs is known in associated liquids, with pairs (molecule associations) held together by hydrogen bonds. This mechanism of association may determine the anomalies in glycerin observed in Ref. [31]. In aromatic liquids, pairs are held together mainly by electrostatic forces. A formal definition of pairing assumes partitioning the two-molecules configuration space into domains corresponding to different pairing situations: the domains (energy basins) surrounding the few relatively deep energy minima represent paired states, and the rest of the configuration space describes unpaired molecules. Details and applications of these ideas are used in the statistical theory of structure recognition (see Ref. [34] and references therein).

For a single dimer at room temperatures, the energy barrier for passing from one energy minimum configuration to another one is only few time the thermal energy

k_BT ($\sim 3k_BT$ in Benzene, see below). Therefore, the lifetime of a single pairing state is only about an order of magnitude larger than the molecular vibration period. When molecules in a cluster pair with more than one neighbor each, the cluster becomes an aggregate of associated molecules. Due to geometrical restrictions, a given pairing state of two molecules limits their possible pairing states with other molecules. A lower energy of packing corresponds to a larger number of pairs in a cluster, and implies a special local order, with correlated positions and orientations of molecules in the cluster. The lifetime of those ordered aggregates substantially increases. The multiplicity of dimer pairing states with close energies allows clusters to have different local orders. We assume that the similar anomalies observed in Benzene, Quinoline, and other liquids reflect changes in the size and statistics of these ordered clusters. The small magnitude of the effects, and apparently the small energies involved, indicate that one deals with a weak association, much weaker than that in associated liquids having strong hydrogen bonding as the primary cause of association. It is important that there is more than one type of pairing, and of low-energy local structure in the liquid. One can see some similarity of the above picture with that of proton disorder in Ice [35].

The most studied aromatic molecule is Benzene. The electronic structure of the Benzene molecule [33] includes a molecular plane with all nuclei and a cloud of s-electrons, and clouds of π-electrons below and above this plane. Interaction energy for two Benzene molecules favors several mutual positions [16,36,37], labeled as T, L, and S configurations. The T-configuration is found in dimers in the gas phase, and in the crystalline phase. In this T configuration, the carbon atom of one molecule is situated near the center of another molecule, and the C-6 axes of the molecules are mutually orthogonal. Another preferred configuration is the L configuration in which a hydrogen atom in one molecule is close to a hydrogen atom and a carbon atom of the other molecule, and the C-6 axes are at right angles. The third known configuration (stacking configuration, S) is when the planes of both molecules are parallel, and there is a small shift of centers along the molecule plane. The calculated [36,37] energy minima for the T, L, and S configurations are -8.5, -6, $-4\,\mathrm{kJ\,mol^{-1}}$, respectively. Using different combinations of T, L, and S pairs in Benzene, one may construct differently ordered clusters with a high number of pairs per molecule. For example, a planar cluster may be built using the T- and L-pairing to produce a layer of the crystalline lattice. In an ordered cluster, the depth of the potential well for the reorientation of a molecule becomes higher, and the lifetime of the local structure in the cluster becomes larger than in a dimer with its single pairing. The large line width of the depolarized Rayleigh lines ($\sim$50–70 GHz) measured in liquid Benzene is probably due to reorientation jumps of molecules between equivalent T configurations in the less ordered parts of the liquid. This line width is about 20 times smaller in Quinoline, indicating deeper energy basins for pairing of two-ring molecules, and leading to reorientation time of about $3 \times 10^{-9}\,\mathrm{s}$. The electronic structure of Quinoline allows one to expect a number of preferred configurations, with energy minima about twice as deep as in Benzene. An additional feature is the asymmetry of the Quinoline molecule due to the nitrogen atom. This asymmetry results in a frozen-in dipole moment, responsible for the large ($\sim$10) dielectric constant of Quinoline.

The electric dipole brings in an additional element of the local order. For pairs of neighboring molecules, this new element is the dipole moment of the pair.

The above description shows that aromatic liquids have a number of pairing states and thus a large number of possible local arrangements in an ordered small cluster of the liquid. The maximum density of pairing (and the minimum of the free energy below the melting temperature) corresponds to the crystalline state. Note that crystalline Benzene is known to have polymorphous transitions. We suggest that close to the melting temperature, at any given time there is a significant concentration of paired molecules and ordered clusters in the liquid having a high number of pairs per particle but made of different combinations of possible pairs. Changes, upon cooling, in appearance frequency and in size of these aggregates describe the ordering on the length-scale next to the size of a molecule. As explained in Refs. [7,8], under certain conditions multiplicity of possible local structures is a prerequisite for a liquid–liquid phase transition. Another possibility is that the phase transition is avoided but the system comes close to a critical state.

One may see similarities and differences between the picture of ordering due to weak association described above, and that of liquid–crystalline ordering. Aromatic molecules containing more than 4 aromatic rings are known to form liquid crystals [38]. The aspect ratio for those molecules is high. In the classical theory of liquid crystals [39], the non-spherical shape of the molecules and high aspect ratio are assumed to cause orientation ordering. We believe that the rich geography of phases in the thermodynamic (T, P)-plane, re-entrance transitions and other features of those liquids suggest the importance of attraction forces and molecular association, and the physical picture of pairing and clustering apply for those systems. The high aspect ratio of the molecules results in easily detectable elements of the local and global order in liquid crystals captured in the order parameter description of nematic, smectic, and other liquid crystalline states. The higher angular moments of anisotropy that may play an important role in systems like Benzene are then neglected because these moments play a secondary role in classical liquid crystals.

Theoretically, one may treat the multi-ring aromatic compounds as a system, with the number of aromatic rings and other details of the chemical structure as new thermodynamic parameters, in addition to the temperature and pressure. Let us denote the set of these parameters as Π, and consider an extended thermodynamic (T, P, Π)-space. The list of known liquid crystals includes liquids with values of Π different but, as one may suggest, not very far from those for Benzene and Quinoline. The singularities in measured properties in known liquid crystals are stronger than those observed in Benzene, Quinoline, and other liquids discussed in our paper, and the liquid–crystalline ordering does not require the rather stringent conditions for observing the anomalies in Benzene and Quinoline. The values that the parameter Π takes in real molecules belong to a discrete set of values. Theoretically, one may interpolate, and consider a continuous set of values for Π. From general considerations one can assume that the free energy landscape in the (T, P, Π)-space does not change abruptly when the coordinate Π is changed from the known liquid crystals towards smaller molecules. Rather, a phase transition surface in the (T, P, Π)-space terminates in a critical point (T_c, P_c, Π_c). The question of

anomalies in the liquids consisting of small organic molecules is then: are these systems "above" the critical value Π_c of Π, and by taking even greater precautions one will arrive at characteristic discontinuities, or these liquids have super-critical values of Π, and the observed anomalies indicate the closest proximity to the critical point T_c, P_c, Π_c. The answer to this question can be found by future experiments.

The anomaly in the heat capacity ratio γ suggests that there is a corresponding anomaly in the thermal expansion coefficient. Local positional and orientational ordering is usually accompanied by volume changes caused by striction (interaction of the order parameters with density). The shape of the anomalies observed in Quinoline is rather typical for near-critical states and other regions of strong fluctuations. The anomaly in hypersound velocity reflects both the fluctuations and the change in the density and short-range order. In a liquid–crystalline transition close to the second order, in addition to direct contributions of fluctuations there are jumps in thermodynamic susceptibilities as predicted by the Landau theory [40], and discontinuities due to the weak first-order nature of the transition. The similarity of the ordering in aromatic liquids and in liquid crystals allows one to expect similarity of manifestations. An anomaly in hypersound velocity in a phase transition in a liquid–crystalline system was observed, for example, in Ref. [41].

One may formally treat an associated low-temperature liquid as a multi-component solution of pairs. Then, the numbers N_α of pairs corresponding to preferred mutual configurations $\alpha = 1,2\ldots$ of molecules become new thermodynamic characteristics of the thermal equilibrium state. In the gas state, and at high temperatures in the liquid, the pair number densities $n_\alpha = N_\alpha/V$ are small. Upon cooling, the fraction of neighboring molecules in preferred mutual configurations increases, and the lifetime of these configurations also increases and becomes significantly larger than the molecular vibration period. When miscibility of components of a multi-component solution is limited, one arrives at non-miscibility-related phase transitions. There is, however, a difference between the systems considered in the classical theory of solutions, and the solution of pairs. In a non-reacting solution, particle numbers of components are conserved quantities, and the chemical potentials for those components depend on temperature, pressure, and particle numbers. In associated liquids, the pair numbers N_α are determined by the conditions of thermodynamic equilibrium, and the formal chemical potentials for pairs are equal zero. Note that the particle number conservation is the cause for the appearance of hetero-phase states in solutions at a phase transition line. For a quasistatic change of the state in associate liquid, there is no component conservation for pairs, and thus no hetero-phase states. However, those states may appear as temporary states when the condition of complete equilibrium are violated by a too rapid (non-quasistatic) change of temperature. In this case, at short times the system behaves as a system with approximately conserved N_α, and may develop a temporary hetero-phase state. This may explain the observation that for insufficient equilibration time, an increased scattering of experimental data is observed rather than a reproducible anomaly (see, for example, Ref. [15]).

An observation that have to be discussed in the framework of the above physical picture is that impurities, and especially dissolved gases, have a strong impact on the

experimental results, diminishing or eliminating the anomalies in aromatic liquids. The electric charge distribution in aromatic molecules creates a complex potential energy landscape. The details of this landscape determine the special pair configurations and corresponding energies. A dissolved Oxygen atom may change this landscape, and thus the energies of pair configurations. This, in turn, influences the parameters determining the phase transition, and thus the shape of the experimental curves. This influence is especially important near the end of the phase transition line. Properties of a system change continuously along a supercritical path in the phase plane, but the rate of changes is substantially increased in the part of the path close to the critical point. The large influence of impurities may indicate that the system is close to a critical point, and impurities shift the critical pressure to higher values. A study of these systems at higher pressures may then give new and more revealing insights into the nature of the observed phenomena.

5. Concluding remarks

Ordering phenomena in different condensed systems substantially differ in the magnitude of manifestations. There are strong ordering processes, (for example, crystallization of simple liquids) with large differences between phases in density, entropy, and other properties. In the liquid–liquid phase transitions, as well as in liquid–crystalline ordering, the energy involved and the magnitude of effects are much smaller. The anomalies in Benzene and Quinoline indicate the existence of even weaker ordering phenomena that are close to a critical situation, and may correspond, as described above, to a phase transition close to a critical point, with very small energy effects, and thus relatively weak anomalies and large relaxation times, or to a supercritical state close to criticality. A distinct and long-living local structure is generally expected in supercooled liquids. The anomalies observed in Benzene, Quinoline, and other aromatic liquids, and the liquid–liquid phase transitions found in molten Bi, Te, and Se, show that at least some liquids have a distinct local structure in equilibrium state above the melting temperature. However, more work is necessary to clarify the intriguing picture of the local ordering in low-temperature complex liquids.

Acknowledgments

AZP acknowledges helpful and insightful discussions with Mark Ratner and Yury Berlin at the Northwestern University.

References

[1] H. Eyring, J. Chem. Phys. 4 (1936) 283.
[2] J. Frenkel, Kinetic Theory of Liquids, Dover, New York, 1955.
[3] V.V. Brazhkin, S.V. Popova, R.N. Voloshin, Physica B 265 (1999) 64.

[4] V.V. Brazhkin, S.V. Popova, R.N. Voloshin, High Pressure Res. 15 (1997) 267.
[5] V.V. Brazhkin, R.N. Voloshin, S.V. Popova, A. Lyapin, Usp. Fiz. Nauk. 169 (1999) 1035.
[6] S. Tamaki, Phase Transit. 66 (1998) 167.
[7] A. Patashinski, A.C. Mitus, B.I. Shumilo, Phys. Lett. 113A (1985) 41.
[8] A.C. Mitus, A. Patashinski, Acta Phys. Pol. A 47 (1988) 779.
[9] K.R. Rao, Curr. Science 80 (9) (2001) 1098.
[10] L. Son, G. Rusakov, N. Katkov, Physica A 324 (2003) 633.
[11] E.W. Fischer, Physica A 201 (1993) 183 and references therein.
[12] S.A. Kivelson, X. Zao, D. Kivelson, T.M. Fisher, C. Knobler, J. Chem. Phys. 101 (1994) 2391.
[13] N.B. Rozhdestvenskaya, L.V. Smirnova, JETP Lett. 44 (1986) 1166.
[14] F.J. Bermejo, M. Garcia-Hernandez, W.S. Howells, R. Burriel, F.J. Mompeán, D. Martin, Phys. Rev. E 48 (1993) 2766.
[15] D. Jalabert, J.B. Robert, H. Roux-Buisson, J.P. Kintzinger, J.M. Lehn, R. Zinzius, D. Canet, P. Tekely, Europhys. Lett. 115 (1991) 435;
J.B. Robert, J.C. Boubel, D. Canet, Mol. Phys. 90 (1997) 399;
L. Gauthier, J.B. Robert, D. Canet, J. Mol. Liq. 85 (2000) 77.
[16] N.B. Rozhdestvenskaya, L.V. Smirnova, J. Chem. Phys. 195 (1991) 1223.
[17] L. Letamendia, M. Belkadi, O. Eloutassi, G. Nouchi, C. Vaucamps, S. Iakovlev, N. Rozhdestvenskaya, L.V. Smirnova, M. Runova, Phys. Rev. E 48 (1993) 3572.
[18] L. Letamendia, M. Belkadi, O. Eloutassi, E. Pru-Lestret, G. Nouchi, J. Rouch, D. Blaudez, F. Mallamace, N. Micali, C. Vasi, Phys. Rev. E 54 (1996) 5327.
[19] M.A. Leontovich, J. Phys. (Moscow) IV (1941) 49.
[20] I.L. Fabelinskii, Molecular Scattering of Light, Plenum Press, New York, 1968.
[21] K. Kawasaki, Physica A 217 (1995) 124.
[22] D. Thirumalai, R.D. Mountain, Phys. Rev. E 47 (1) (1993) 479.
[23] C.K. Bagdassarian, D.W. Oxtoby, J. Chem. Phys. 100 (1994) 2139.
[24] X. Zhao, D. Kivelson, J. Phys. Chem. 99 (1995) 6721.
[25] D. Kivelson, S.A. Kivelson, Xiaolin Zhao, Z. Nussinov, G. Tarjus, Physica A 219 (1995) 27.
[26] W. Ellison, B. Agnus, R. Vicq, G. Delbos, Second Liquid Matter Conference, Firenze Italy, September 1993
B. Agnus, Ph.D. Thesis, Bordeaux, unpublished, 1994.
[27] E. Zamir, N.D. Gershon, A. Ben-Reuven, J. Chem. Phys. 55 (1971) 3397.
[28] B.J. Berne, R. Pecora, Dynamic Light Scattering, Wiley-Interscience, New York, 1975.
[29] J.P. Boon, S. Yip, Molecular Hydrodynamics, Mc-Graw Hill, New York, 1980.
[30] B. Quentrec, Ann. Phys. (Fr.) 9 (1984) 1.
[31] M. Grimsditch, N. River, Appl. Phys. Lett. 58 (1991) 2345.
[32] A.Z. Patashinski, M.A. Ratner, J. Chem. Phys. 120 (2004) 2814.
[33] R.T. Morrison, R.N. Boyd, Organic Chemistry, Prentice-Hill, Englewood Cliffs, NJ, 1992.
[34] A. Patashinski, A. Mitus, M. Ratner, Phys. Rep. 288 (1997) 409.
[35] D. Eisenberg, W. Kauzman, The Structure and Properties of Water, University Press, New York, Oxford, 1969.
[36] L.D. Lowden, D. Chandler, J. Chem. Phys. 61 (1974) 5228;
L.D. Lowden, D. Chandler, J. Chem. Phys. 59 (1973) 6587.
[37] P. Linse, J. Am. Chem. Soc. 106 (1984) 5425;
Shi Xiangian, L.S. Bartell, J. Phys. Chem. 92 (1988) 5667.
[38] D. Demus, J. Goodby, G.W. Gray, H.-W. Spiess, V. Vill (Eds.), Handbook of Liquid Crystals, vol. 4, Wiley-VCH, Weinheim, New York, Chichester, Brisbane, Singapore, Toronto, 1999.
[39] S. Chandrosekhar, Liquid Crystals, Cambridge University Press, Cambridge, 2002.
[40] L.D. Landau, E.M. Lifshitz, Statistical Physics Part I, Pergamon, New York, 1988.
[41] G. Durand, A. Narasimha, Phys. Lett. 27A (7) (1968) 455.